Effect of Cu Addition on Delayed Fracture Resistance of Low Carbon 1470 MPa Grade Thin-walled Martensite Steel

Shunsuke Toyoda[1], Jun'ichi Sakai[2]

[1] The Japan Society for Heat Treatment, [2] Kagami Memorial Res. Inst. for Mater. Sci. and Technol. of Waseda University

The effect of chemical composition on delayed fracture resistance was investigated. Chemical composition of the base steel alloy was 0.18%C-0.4%Si-1.8%Mn-0.015%Nb-0.01%P-0.001%S. Cu, Ni, Cr, B and Mo were individually added to the base steel. A 4-point bending test in 1 N-hydrocrolic acid was conducted for quench and tempered specimens. Cu added steel showed the best delayed fracture resistance. After the immersion, a metallic Cu layer was formed on the steel surface.

To clarify the effects of the addition of Cu on the suppression of hydrogen embrittlement in a solution of HCl, hydrogen permeation tests and dynamic polarization measurements were conducted on TS 1470 MPa grade, low-carbon martensite steels. To this end, steels containing 0.19% C, 0.2% Si, 1.3% Mn, Cr, Ti, Nb and B were prepared with and without 0.16% Cu. The results of hydrogen permeation tests indicated that the steady-state hydrogen permeation current (J_H) of steel containing 0.16% Cu was considerably lower than that of basic steel in 0.1 N HCl at the corrosion potential. Moreover, the J_H of martensite steel was suppressed by the addition of Cu, and the cathode current, (i_C) and the J_H/i_C were reduced. The results obtained in this study corroborated the hypothesis that the 1 or 2-μm metallic Cu particles precipitated on the surface of the steel in a solution of HCl suppressed the cathodic reaction and the introduction of hydrogen.

To clarify the effects of Cu addition on hydrogen absorption and diffusion properties of steel under atmospheric condition, corrosion test was conducted on a 1470 MPa grade thin-walled low carbon martensite steel tube. A martensite steel tube bearing 0.18% C, 0.4% Si, 1.5% Mn, 0.15% Cu, 0.01% Nb was prepared and compared with Cu free steel tube. As a result of EPMA mapping for the rust layer, Cu accumulated discretely on the rust/steel interface, especially in the bottom of pits of 0.15% Cu bearing steel tubes. According to x-ray absorption near-edge structure (XANES) spectra, the valence of Cu in the rust layer was mainly +2 as Cu- (O, OH, SO$_4$). The average and maximum diffusible hydrogen content level of 0.15% Cu bearing steel was lower than that of Cu free steel after the atmospheric corrosion test. Having regard to the fact that the valance of Cu could also be 0, an inhibition mechanism from accumulated Cu on hydrogen-induced cracking was proposed. Eluted Cu^{y+} ions in the rust layer may precipitate as metallic Cu at the microscopic cathode during the corrosion test. As a result, the microscopic cathode becomes inactivated as an electrochemical reaction site for hydrogen. The Cu alternates between precipitates and Cu ions depending on the relative humidity, and the condensation and pH of the water in the rust layer.

1. Introduction

The latest problem of automotive maker is energy efficiency of vehicles in order to preserve the environment. One of the methods to solve this problem is weight reduction of automobiles by using high-strength steels. For the automotive structural parts, many of practical properties, such as formability, low temperature toughness, weldability, and the delayed fracture resistance, which is closely related to diffusible hydrogen, are required.

In this study[1,2,3], in view of improvement of delayed fracture resistance, the effects of Cu addition on hydrogen absorption and diffusion properties of 1470 MPa grade thin-walled low carbon martensite steels are investigated.

2. Experimental procedure

Firstly, to evaluate the effects of additional elements on delayed fracture resistance of martensite steel sheets, 4-point bending test was conducted in 1N-hydrochloric acid[1]. The chemical composition of base steel used was 0.18%C-0.4%Si-1.8%Mn-0.01Nb-0.01%P-0.01%S and Cu, Ni, Cr, B and Mo were individually added. 2mm thick cold-rolled steel sheets were heat-treated at 870℃ for 5 min in salt bath, water quenched and tempered at 200℃ for 5 min. The tensile strength was ranged from 1457 to 1542 MPa. To elucidate the mechanism of delayed fracture suppression by Cu addition, diffusible hydrogen after immersion in 1.6N-hydrochloric acid for 0.5h was measured by thermal desorption analysis.

Secondly, to consider the hydrogen entry suppression effect by Cu under hydrochloric acid condition by electrochemistry, hydrogen permeation tests and dynamic polarization measurements were conducted. 0.19%C-0.2%Si-1.3%Mn-0.2%Cr-Ti, Nb, B based steel and 0.2% Cu added steel sheets were used in the measurements. Specimen was heated at 950℃ for 5 min, water quenched, and tempered at 200℃ for 5 min. Hydrogen permeation tests were conducted in solution of HCl at the corrosion potential. The environmental side of the cell was filled with deaerated 0.1N HCl, and the hydrogen detection side was filled with deaerated 0.1N NaOH. Prior to the test, the surface of the hydrogen detection side was electroplated with NiCl$_2$, NiSO$_4$, H$_3$BO$_3$ solution at -10 mA/cm^2 for 120s. The hydrogen detection side was polarized at a constant potential of +100mV (vs. SCE) for prompt ionization of permeated hydrogen atoms. To determine the hydrogen diffusion constant D_{eff}, hydrogen permeation tests and were conducted under a potential gradient. Dynamic polarization measurements were also conducted in deaerated 0.1N HCl with working electrode.

Finally, to clarify the effects of Cu addition on hydrogen absorption and diffusion properties under atmospheric corrosion, atmospheric corrosion test was conducted on 1470 MPa grade thin-walled steel tube[3]. Base steel tube (0.17%C-0.4%Si-1.8%Mn-Nb) and Cu added steel tube (0.18%C-0.4%Si-1.5%Mn-0.15%Cu-Nb, Ti, B) were prepared. The tube size was 31.8 mm in diameter, 2.0 mm in thickness and 150 mm long. The tubes were exposed mor than 12 years under atmospheric corrosion condition in a coastal industrial zone without electro-deposition coat. The amount of air born NaCl was about 0.07 mg/dm^2/day. After the atmospheric corrosion test, the rust layer of the tube sample was characterized with EPMA, X-ray Absorption

Fine Structure (XAFS) analysis. Diffusible hydrogen in steel tube body was evaluated by TDS after the corrosion test.

3. Results and discussion

3.1 Effect of Cu addition on delayed fracture resistance in hydrochloric acid

Figure 1 shows the time to fracture and the corrosion rate in 1N-hydrochloric acid of 4-point bending tested specimen. Corrosion rate was evaluated after immersion test in 1N-hydrochloric acid without loading stress for 400h. 1.8Mn-Cu specimen showed a much higher delayed fracture resistance and a lower corrosion rate than 1.8Mn base steel. After the 1N-hydrochloric acid immersion test, metallic Cu particles, whose diameter was 1 or 2 μm, were dispersed on the surface observed by SEM. It is assumed that deposited Cu particles suppress cathodic reaction and hydrogen entry at the specimen surface.

Figure 2 shows hydrogen evolution profiles during continuous heating measured by thermal desorption analysis of copper containing and not containing martensite steel sheets after immersion in 1.6N-hydrocrolic acid for 0.5h. The diffusible hydrogen, corresponding to evolution below $200^{\circ}C$, of Cu containing steel was 0.006 ppm, which was much lower than not containing steel sheets of 0.031 ppm. This indicates hydrogen entry suppression effect by Cu under hydrochloric acid condition.

3.2 Effect of Cu addition on hydrogen absorption and diffusion properties in solution of HCl

Figure 3 shows the time dependence of the hydrogen permeation current J_H of martensite steel in solution of HCl at the corrosion potential. This result indicated that the J_H of base steel increased over time and reached constant value. On the other hand, the J_H of Cu added steel reached maximum value and decreased gradually until a steady-state J_H of was achieved. The steady-state J_H of Cu added steel was considerably lower than that of base steel.

From the results of the hydrogen permeation tests, D_{eff} was calculated. D_{eff} of base martensite steel and Cu added steel were the same value of 2.6×10^{-6} cm^2/s.

Figure 4 shows the polarization behavior of martensite steel in 0.1N hydrochloric acid. The results revealed the cathodic and anodic polarization curves were affected by the addition of Cu. The polarization current neighborhood of the corrosion potential was decreased by Cu addition.

3.3 Effect of Cu addition on hydrogen absorption and diffusion properties under atmospheric corrosion

Figure 5 shows the EPMA mapping of Cu added martensite steel tube surface. Cu accumulated discretely on the rust/steel interface, especially in the bottom of pits. As discussed in later, this may be a precipitated metallic Cu from the eluted Cu^{y+} ion in condensed water layer that was emerged during atmospheric corrosion on the tube surface. This accumulation is expected from inhabitation of the pitting growth and hydrogen entry at the points where Cu exists.

Figure 6 shows Cu-K edge XANES spectrum recorded for rust powder scraped off from Cu added steel tube surface exposed over 12 years with spectra for polished Cu added steel tube surface. The spectra measured for some reference materials are also indicated in the figure. Extended x-ray absorption fine structure (EXAFS) analysis for Cu on polished Cu added steel tube surface revealed that Cu atom in the bulk dissolve d mainly in the state of substitutional solid solution in bcc-Fe structure. The edge position of the spectrum for the rust was higher than that for the polished surface and Cu metal foil, which showed that the Cu in the rust layer was oxidized. By comparing the edge position of XANES spectra, it would appear that the valence of Cu in the rust was mainly +2. However, the XANES spectrum differs from those of the reference materials with divalent Cu. The spectrum is somewhat close to those of CuO and CuSO$_4$ rather than those of CuS and CuCl$_2$. The EXAFS analysis showed that oxygen is the nearest neighbor atom of Cu in the rust. So, it is considered that the dominant chemical state of Cu atom was Cu-(O, OH, SO$_4$) in the rust layer.

Figure 7 shows a schematic illustration of the inhibition mechanism of accumulated Cu on hydrogen-induced cracking when a water condensation occurs after years of atmospheric corrosion. This mechanism explains well the inhibiting effect of Cu addition on delayed fracture resistance. X-mark indicates the inhibited reaction and cracking by Cu precipitation on the microscopic cathode, such as emerged sulfide.
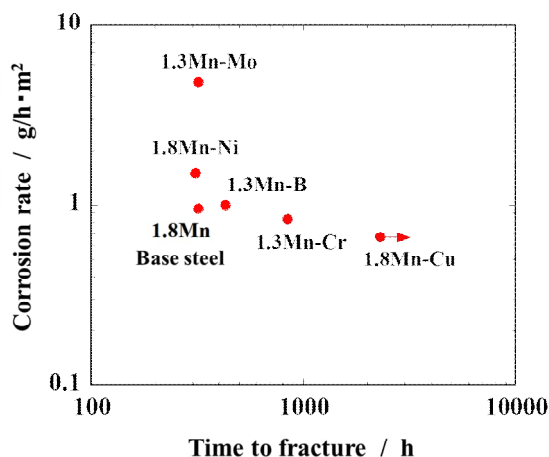

Figure 1. Time to fracture of 4-point bending test and the corrosion rate in 1N-hydrochloric acid
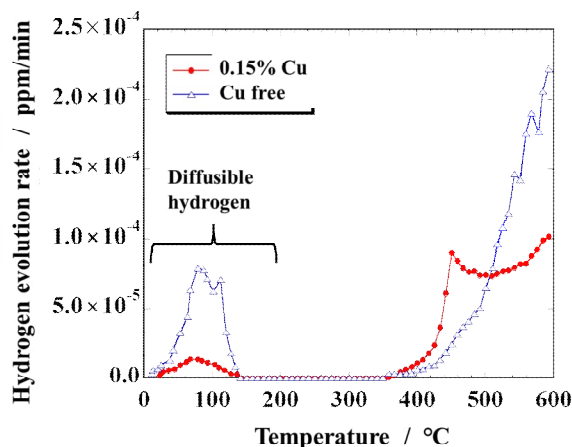

Figure 2. Hydrogen evolution profiles during continuous heating measured by TDA after immersion in 1.6N-hydrochloric acid for 0.5h.
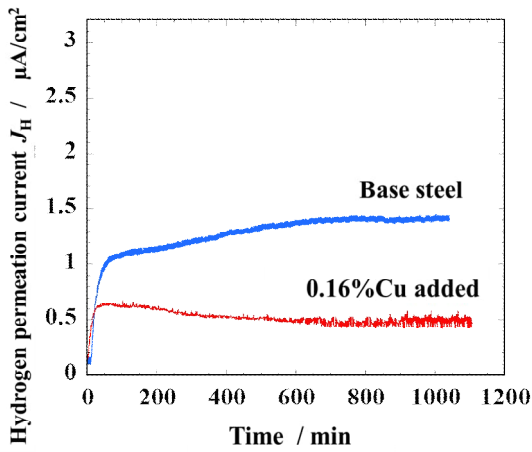
Figure 3. Time dependence of the hydrogen permeation current of martensite steel in solution of HCl

Figure 4. Polarization behavior of martensite steel in 0.1N hydrochloric acid

Figure 5. Compositional mapping of Cu added martensite steel tube surface
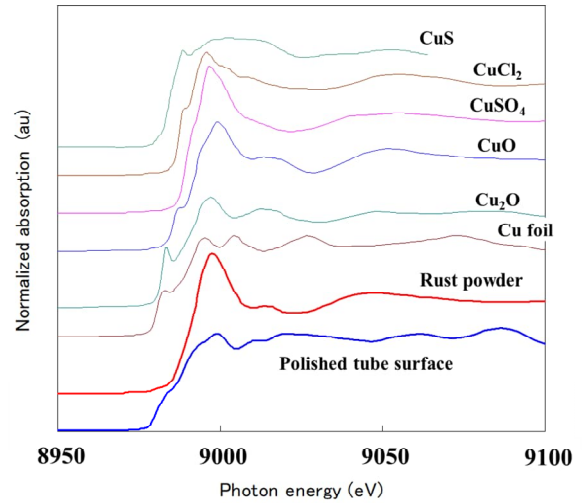

Figure 6. Cu-K edge XANES spectrum recorded for rust powder scraped off from Cu added steel tube surface exposed over 12 years under atmospheric environment
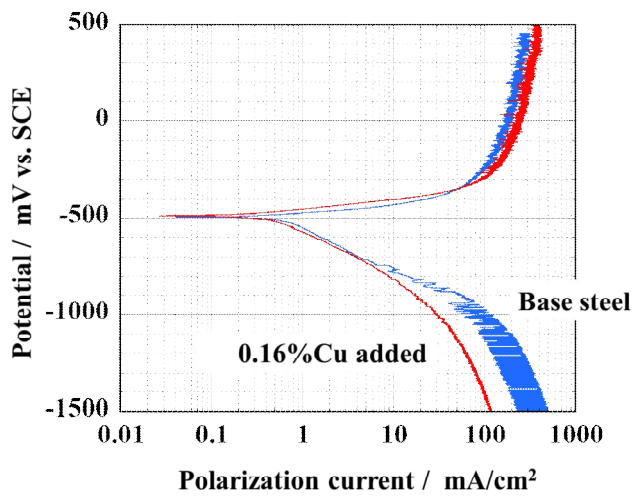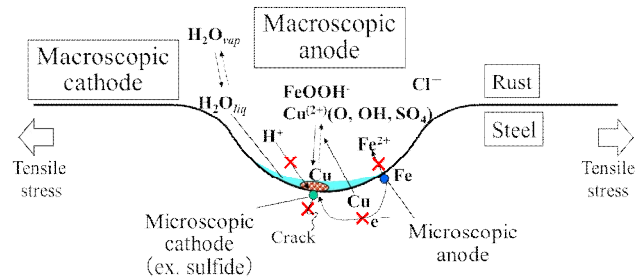

Figure 7. Schematic illustration of the inhibition mechanism of accumulated Cu on hydrogen-induced cracking

4. Conclusions

Cu-added steel showed excellent delayed fracture resistance in hydrochloric acid immersion condition. After the immersion, metallic Cu layer was formed on the steel surface. Cu addition also lowered the corrosion rate in hydrochloric acid.

In hydrogen permeation tests conducted in 0.1N HCl at the corrosion potential, the steady state hydrogen permeation current J_H of steel containing 0.16% Cu was considerably lower than that of base steel.

Cu was accumulated discretely at the rust/steel interface, especially in the bottom of pits of 0.15% Cu bearing steel tube after the atmospheric corrosion test. According to the XAFS spectra, the valence of Cu in the rust layer was mainly +2 as Cu-(O, OH, SO$_4$).

Acknowledgments

References
1) S. Toyoda, Y. Ishiguro, Y. Kawabata, K. Sakata, A. Sato and J. Sakai: *ISIJ Int*. 48-5, (2008), pp. 640-648
2) S. Toyoda, H. Kimura, Y. Kawabata, Y. Yamane and J. Sakai: *ISIJ Int*. 51-3, (2011), pp. 456-461
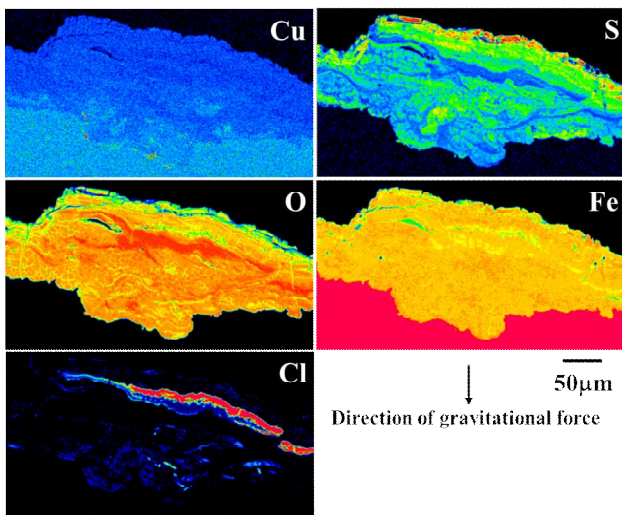3) S. Toyoda, H. Kimura, M. Nagoshi, I. Kage, N. Yoshihara and J. Sakai: *ISIJ Int*. 51-9, (2011), pp. 1516-1523